J. Phys. Chem. Lett., **2013**, 4, 2715-2720 DOI: 10.1021/jz4014085

Plasmonic Mesoporous Composites as Molecular Sieves for SERS Detection

Vanesa López-Puente,[1] Sara Abalde-Cela,[1] Paula C. Angelomé,[1,2] Ramón A. Alvarez-Puebla,[3,4,5] and Luis M. Liz-Marzán[1,6,7,*]

[1] *Departamento de Química Física, Universidade de Vigo, 36310 Vigo, Spain*

[2] *Gerencia Química, Centro Atómico Constituyentes, Comisión Nacional de Energía Atómica, Av. Gral Paz 1499, B1650KNA, San Martín, Buenos Aires, Argentina*

[3] *Departamento de Quimica Fisica e Inorganica, Universitat Rovira i Virgili, Avda. Països Catalans 26, 43007 Tarragona, Spain*

[4] *Centro de Tecnologia Quimica de Cataluña, Carrer de Marcel•lí Domingo s/n, 43007 Tarragona, Spain*

[5] *ICREA, Passeig Lluís Companys 23, 08010 Barcelona, Spain*

[6] *Bionanoplasmonics Laboratory, CIC biomaGUNE, Paseo de Miramón 182, 20009 Donostia - San Sebastián, Spain*

[7] *Ikerbasque, Basque Foundation for Science, 48011 Bilbao, Spain*

*** Corresponding author e-mail:** llizmarzan@cicbiomagune.es

ABSTRACT

Application of surface enhanced Raman scattering (SERS) spectroscopy to the ultrasensitive analysis of small molecules in biological samples is complicated by signal contamination by ubiquitous macromolecules such as proteins, nucleic acids or lipids. We present a proof-of-concept study of the application of composite films comprising branched gold nanoparticles embedded in mesoporous thin films, which act as molecular sieves. The inorganic mesoporous layer only allows the diffusion of small molecules toward the plasmonic particles while preventing the contact of macromolecules in solution with the optical sensor.

Keywords: SERS, gold nanoparticles, mesoporous films, molecular sieves, biodetection, biosensing

TOC Graphic

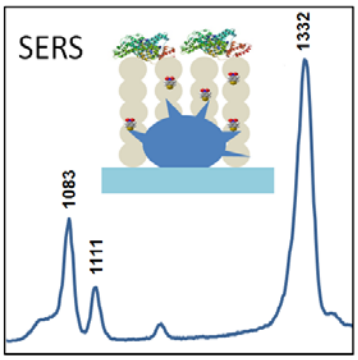

Application of surface enhanced Raman scattering (SERS) spectroscopy to the analysis of biological fluids[1] is severely constrained by the non-specific adsorption of molecules present in the matrix solution onto metallic nanostructures. This retention processes can block the adsorption of the target analytes and/or increase the difficulty of vibrational assignment.[2,3] Therefore, it is imperative to design novel enhancing substrates that can restrict the competitive adsorption of non-relevant molecules. In the case of biofluids, these molecules are typically rather large, such as proteins, nucleic acids or lipids, and thus they can potentially be excluded from the substrate by sieving, i.e. by placing a protective filtering material on the metal nanostructures, while maintaining a high plasmonic enhancement. In this respect, mesoporous materials[4-6] present a great potential, since they contain highly ordered and monodisperse pores in the size range of 2–50 nm,[5] so that the size exclusion limit can be tuned at will. Numerous examples can be found in the literature regarding the combination of mesoporous oxide thin films with metallic nanoparticles,[7-17] prepared either by direct nanoparticle synthesis inside a preformed porous oxide, or by incorporation of preformed nanoparticles in the precursor solution of the mesoporous thin film. The latter method allows a better control over the initial shape and spatial localization of the nanoparticles. However, certain morphologies, such as those comprising thin branches or spikes, are difficult to preserve during mesoporous film formation, mainly because of the high temperatures involved, which may lead to nanoparticle reshaping.[18] We have recently reported the synthesis of branched gold nanoparticles within mesoporous silica films, through seeded growth, templated by the pores in the film.[19] This kind of nanoparticles are particularly interesting, as it has been demonstrated that such features provide them with a high sensitivity toward local changes in their dielectric

environment,[20] as well as the ability to generate large electric field enhancements,[21] rendering them ideal for SERS applications.[22] In the context of biochemical analysis, these composite substrates in which Au nanoparticles are fully covered with mesoporous thin films, are expected to prevent macromolecule adsorption and, in turn, signal interference by the size restriction imposed by the small pores.[23] We present here the preparation of a composite material formed by a mesoporous thin film containing gold nanoparticles, which is SERS active and stable under biological conditions. By taking advantage of the mesoporous nature of the film, a proof-of-concept size exclusion experiment was designed to demonstrate that the mesoporous film can indeed act as a molecular sieve for biofluids, preventing the diffusion of big proteins inside the matrix while allowing the diffusion of small molecules of interest that can be detected by SERS spectroscopy.

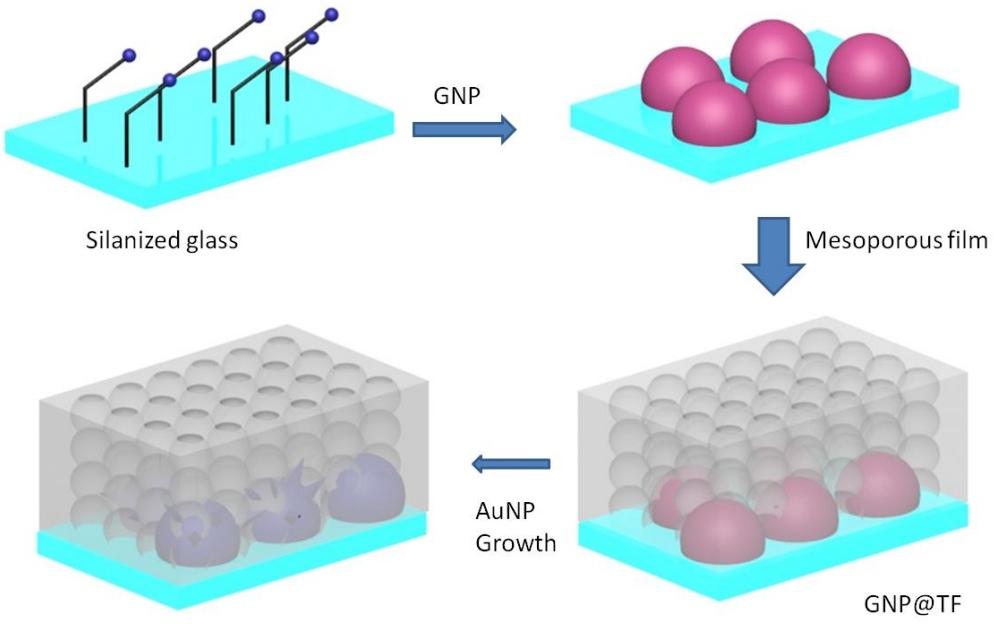

Figure 1. Schematic representation of the synthetic process. Gold nanoparticles are attached onto a silanized glass slide, through amine binding; then a mesoporous film is deposited on top and spikes are grown from the nanoparticles, using the pores as templates. Not drawn at scale.

The synthetic procedure is based on a recently reported two-step protocol.[19] The first step comprises the attachment of Au nanoparticles onto glass slides modified with aminopropyl-trimethoxysilane (APS), so that pre-synthesized citrate-stabilized gold nanoparticles bind chemically on the glass surface via the amino-terminated silanes.[24] Once the nanoparticles were effectively attached onto the glass surface, SiO_2 or TiO_2 (using the corresponding precursors) mesoporous films were deposited by spin coating using block copolymer Pluronic F127 micelles as templates and placing them in a 50% relative humidity chamber to facilitate evaporation induced self-assembly. A consolidation step was then applied by slow heating through two successive 24h heat treatments at 60 ºC and 120 ºC, respectively, and a final 2h step at 200 ºC to lock the structure, eliminating undesired microporosity by enhancing the microphase separation of the template, and leading to complete inorganic condensation. Finally, the films were immersed in ethanol for 3 days to remove the organic template. The Au nanoparticles (two different sizes were used, 15 and 80 nm diameter) were perfectly localized at the substrate-film interface, as they were initially adsorbed onto the substrate by strong interactions that were not affected by thin film preparation, as previously reported.[25] The second step comprises the seed-mediated growth (see details in the Experimental Section) of the nanoparticles through the mesoporous thin film, using the pores themselves as templates to produce sharp tips over the initial spherical nanoparticles,[19] which was expected to improve the SERS efficiency of the material.

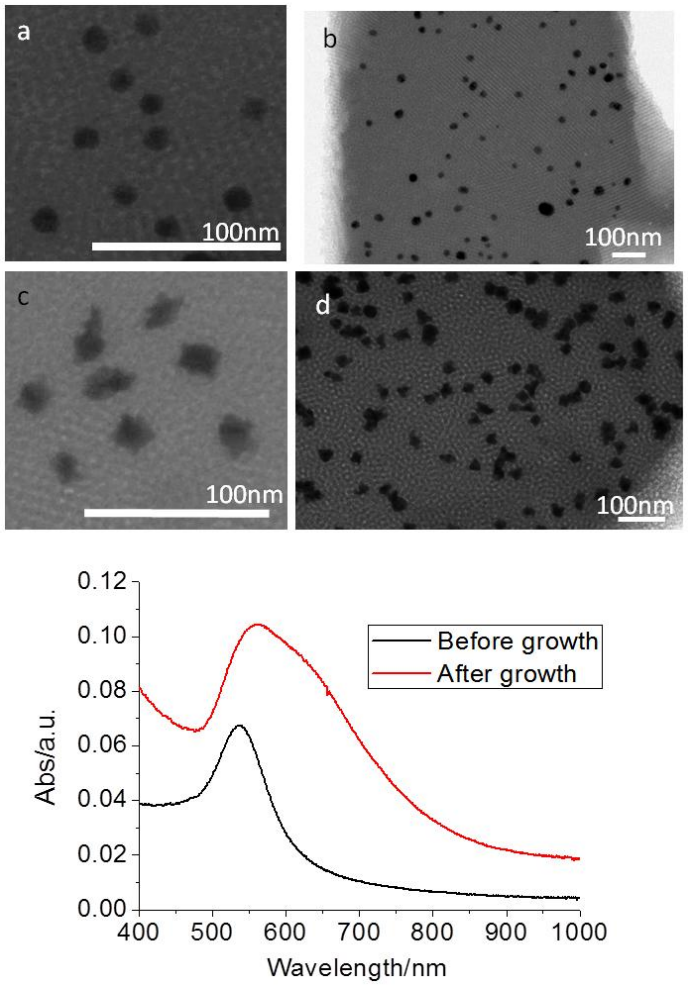

Figure 2. TEM images before (a,b) and after 6h of seeded growth reaction (c,d) for 15nmGNP@TF samples. e) UV-vis-NIR spectra of 15nmGNP@TF samples before and after growth from a CTAB:AA:Au solution with 60:16:1 molar ratio.

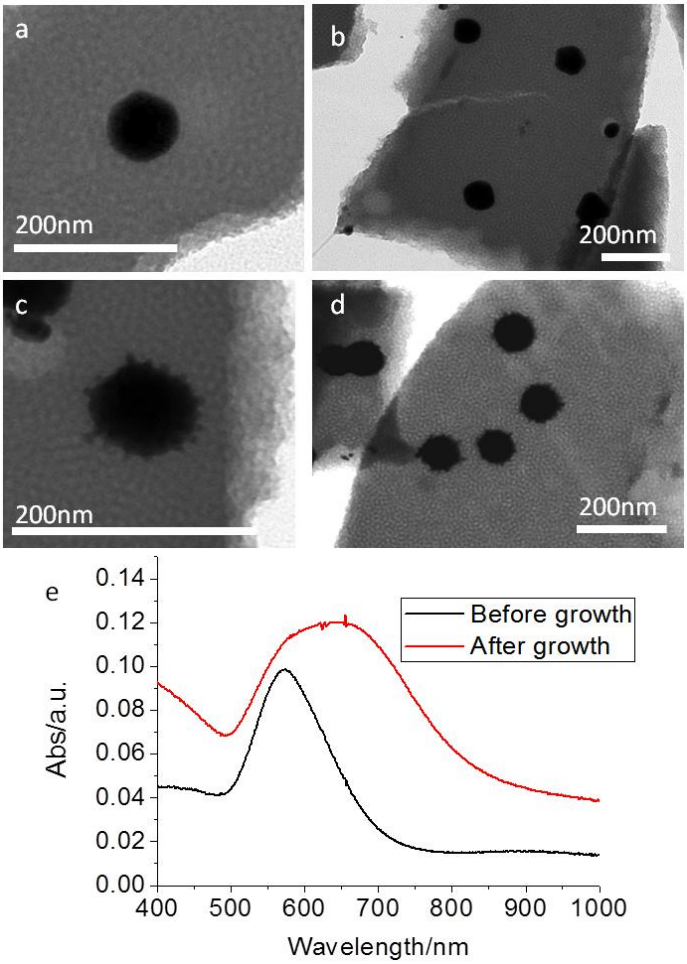

Figure 3. TEM images before (a,b) and after 6h of seeded growth reaction (c,d) for 80nmGNP@TF samples. e) UV-vis-NIR spectra of 80nmGNP@TF samples before and after growth from a CTAB:AA:Au solution with 60:16:1 molar ratio.

In all samples, uniform and highly organized films were obtained (note that the order may not be apparent in TEM images because of misalignment of the mesocrystalline pore structure). Synthetic conditions were chosen to produce mesoporous thin films with ordered pores in an *Im3m* cubic phase, with [110] planes oriented parallel to the substrate, which is the commonly obtained phase when templating with F127.[26] The interpore distances (from center to center of adjacent pores, thus including pore

diameter and wall thickness) were measured from TEM images, obtaining identical values of 12 nm for both mesoporous silica (SF) and titania (TF) thin films. The film thickness was measured from SEM cross-section images, yielding layer thicknesses of 130±6 nm for TF and 95±5 nm for SF. Gold nanoparticle growth (and branching) through the mesoporous thin films was evaluated by TEM and UV-vis-NIR spectroscopy (Figures 2, 3). Before growth (Figures 2a,b and 3a,b), the particles were found to be spherical and uniformly dispersed within the film for both 15 and 80 nm samples. However, after growth (Figure 2c-d and 3c-d and S1, Supporting Information), small tips can be readily seen along the pores in contact with the initial nanoparticles, yielding branched morphologies that are difficult to obtain using traditional colloid chemistry methods. Shown in Figures 2e and 3e are the UV-vis-NIR spectra of TF composite films before and after tip growth (see also Figure S2, SI, for SF samples). Whereas the LSPR bands for the composite SF films are centered at 527 and 556 nm for 15 and 80 nm nanoparticles respectively, in the TF films they are located at 538 and 573 nm for 15 and 80 nm particles, respectively. This shift is due to the increased refractive index around the particles, from n=1.321 (for SF) up to 1.662 (for TF), as determined by ellipsometry. After 6h of immersion in the growth solution, a second band is observed at longer wavelengths, revealing the presence of a second LSPR mode, related to the branches, as previously reported for Au nanostars.[21,22,27] The intensity of the tip LSPR band was found to be higher for SF than for TF samples, due to a larger amount and length of the formed tips, as observed in the corresponding TEM images (Figure S1, SI). It is also important to note the more anisotropic shape of particles under the silica mesoporous thin film. Optimization of the seed-mediated growth conditions was carried out with 15nmGNP@TF samples by using different AA:Au and CTAB:Au molar ratios.

The application of these composite films as SERS substrates requires chemical stability in aqueous (biological) environments, which may be compromised when mesoporous silica is used.[28] To this end, we prepared a simulated biological medium by simply dissolving bovine serum albumin (BSA) in phosphate buffered saline (PBS), and the stability of both titania and silica films was tested by storing them in this solution overnight. TEM observation showed that silica mesoporous films lost their integrity (Figure S3, SI), whereas titania films apparently remained intact. Both titania and silica composite films were evaluated as SERS substrates, so that the SF samples could be used as a control to demonstrate the filtering activity of TF films by size exclusion. The SERS efficiency was tested for the Au nanoparticles of two different sizes, 15 and 80 nm (see Table S1 and Figure S4, SI). A standard Raman molecular probe, 4-nitrobenzenethiol, was used for the SERS evaluation. A portion of about 0.5×0.5 cm^2 of each film was immersed in a 10^{-5} M 4-NBT solution in PBS, and subsequently air-dried and characterized with three different excitation laser lines in the red (633 nm) and near-IR (785, 830 nm). In all cases, strong SERS signals corresponding to the characteristic vibrational bands of 4-NBT were acquired (Figure 4d): CS stretching (723 cm^{-1}), CH wagging (854 cm^{-1}) and CH bending modes (1083 cm^{-1}, 1110 cm^{-1}, 1143 cm^{-1}).[29] Notably, PBS was not detected in any of the samples due to its extremely low SERS cross-section.[30] Comparison of the SERS intensities of 20 acquired spectra per sample showed that the most efficient substrates were those containing 80 nm nanoparticle cores (80nmGNP@TF), due to the generation of stronger electric near field enhancements for larger nanoparticles,[31,32] when the growth solution was Au:CTAB:AA 1:60:16. (Figure S4, SI).

We thus used these substrates for a proof-of-concept experiment to probe their bioanalytical applicability. The size exclusion ability of the mesoporous films when

analyzing complex matrices was demonstrated with bovine serum albumin (BSA) as a simplified biological medium system. Figure 4A shows the SERS spectrum of 80nmGNP@SF after immersion in a BSA (PBS) solution for 18 hours. In agreement with the above-mentioned low stability of SF films in PBS (Figure S3, SI) the mesoporous film was partly dissolved during the experiment. As a consequence, the BSA characteristic vibrational bands were registered in this control experiment due to the interaction of the proteins contained in BSA with the gold nanoparticles, for example the CS stretching (637 cm^{-1}) the thiolated Cys and Met, Tyr (830 cm^{-1}) or Phe (1003 cm^{-1}, 1036 cm^{-1} and 1250 cm^{-1}).[33,34] In contrast, when the same experiment was carried out using 80nmGNP@TF, no BSA Raman signal was recorded, thereby demonstrating the stability of the titania films in biological media. An additional control experiment was carried out with a solution prepared by dissolving 4-NBT (10^{-5} M) in a BSA solution (50 mg/mL in PBS, in the range of albumin concentration in human serum), as a characteristic bio-sample for SERS analysis. When a piece of SF sample was immersed in the bio-sample containing 4-NBT, BSA and PBS, dissolution of the SF mesoporous film was again revealed by the presence of 4-NBT and BSA characteristic signals in the obtained SERS spectra (Figure 4B). However, the TF mesoporous films showed again size selective detection, as can be seen by comparing the spectra of a pure 4-NBT solution (Figure 4C) with that of the bio-sample containing 4-NBT, BSA and PBS (Figure 4D). This is attributed to the presence of pores and necks between the pores in the film that are too small to allow BSA diffusion down to the gold nanoparticles surface. Specifically, the hydrodynamic diameter of BSA is ca. 7 nm, whereas the pore size of the titania mesoporous thin film prepared by this method is around 6 nm, and the necks between the pores are even smaller,[35,36] thereby allowing 4-NBT to diffuse through the pores of the mesoporous film and reach the branched gold

nanoparticles, thus being exposed to the electromagnetic field produced during laser irradiation. As a result, the SERS spectrum (Figure 4D) shows the characteristic signals for 4-NBT, without contamination from BSA, as found in the control experiments when using silica mesoporous films (Figure 4B).

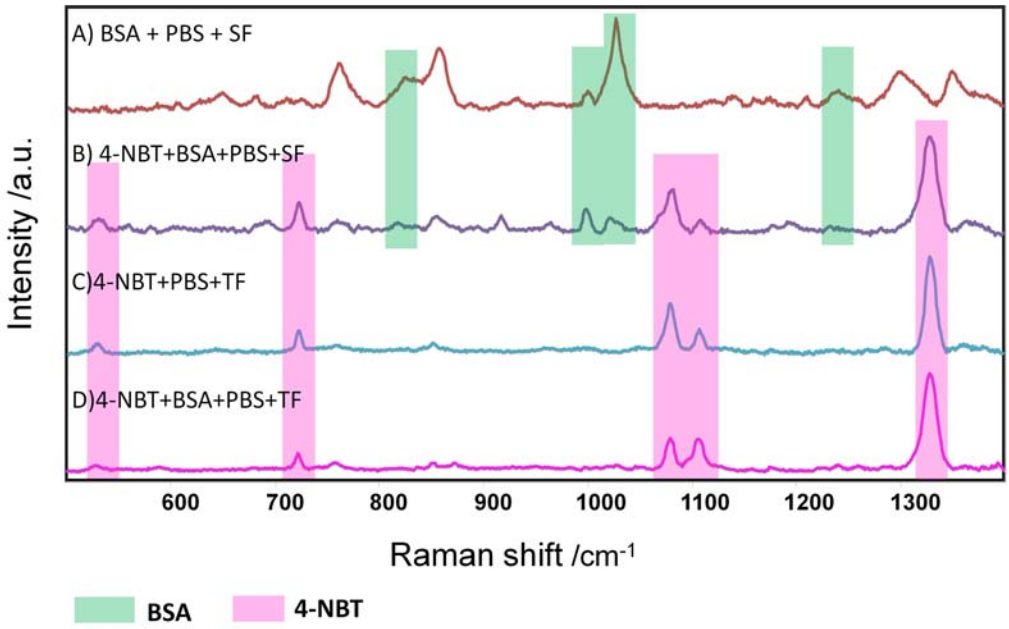

Figure 4. SERS spectra from 80nmGNP with different films and compositions showing the size exclusion proof-of-concept. (A) Spectrum of BSA on SF samples in PBS; B) Spectrum of 4-NBT on SF samples, in the presence of BSA and PBS; C) Spectrum of 4-NBT on TF samples, in the presence of PBS; D) Spectrum of 4-NBT on TF samples, in the presence of BSA and PBS.

In summary, we have demonstrated the fabrication of a novel SERS substrate comprising a sub-monolayer of gold nanoparticles covered with a mesoporous thin film, which can act as a molecular sieve by size exclusion and avoid contamination of SERS

spectra in biological media. The seeded growth of the nanoparticles through the mesoporous film allowed the formation of sharp tips, which improved the SERS efficiency of the material. The obtained composite materials combine the interesting optical properties of metal nanoparticles with the filtering ability and chemical stability of mesoporous titania thin films. Simulating the composition of human serum, a proof of concept size exclusion experiment was designed to evaluate the analytical application of TF and SF composite films. The results presented in this work clearly demonstrate that titania mesoporous thin films can act as molecular sieves in biological media, restricting the diffusion of large molecules (proteins) while allowing the diffusion of small molecules of interest that can be detected by SERS. The multiplex potential of SERS, together with the possibility of in situ monitoring, pave the road toward real time determination of relevant metabolites directly in bioexperiments with no need of manipulating samples, as is the case in imunoanalytical methods.

Experimental

Materials: Tetrachloroauric(III) acid trihydrate ($HAuCl_4 \cdot 3H_2O$), trisodium citrate dihydrate, HCl (conc.), tetraethylorthosilicate (TEOS), $TiCl_4$, (3-aminopropyl)trimethoxysilane (APS), 4-nitrobenzenethiol (4-NBT), hydrogen peroxide 28% (H_2O_2) and sulfuric acid 98% (H_2SO_4) were supplied by Aldrich. Phosphate Buffer Saline (PBS), Bovine Serum Albumin (BSA), Pluronic F127 ($HO(CH_2CH_2O)_{106}(CH_2CH(CH_3)O)_{70}(CH_2CH_2O)_{106}OH$) and ascorbic acid (AA) were purchased from Sigma. Cetyltrimethylammonium bromide (CTAB) was supplied by Fluka. All chemicals were used as received. Pure grade ethanol and Milli-Q water were used as solvents.

Particle preparation. Citrate-stabilized Au spheres (15 nm diameter) were synthesized by using the Turkevich[37] method and used without purification. Citrate-stabilized Au spheres (80 nm diameter) were prepared according to a previously reported procedure and used without purification.[38]

Glass preparation. Glass slides were washed in piranha solution for 30 min, then copiously rinsed with pure water and stored under water until use. The surface was silanized by dipping the dry glass slides in a 0.01 M (in ethanol) solution of APS for 3h and then rinsed with ethanol. Next, the glass slides were immersed in the Au nanoparticles solution for 10 min.

Preparation of mesoporous films. Titania and silica mesoporous thin films were produced by spin-coating 125 μL of the precursor solution on top of the gold nanoparticles modified glass slides, at a spinning rate of 4000 rpm. The technique was based on the evaporation induced self-assembly (EISA) strategy using an inorganic precursor and a surfactant template in ethanol solution. Detailed sol preparation techniques were reported elsewhere.[26,39,40] TEOS and $TiCl_4$ were used as the inorganic precursors and Pluronic F127 was selected as a template. For the mesoporous titania films, the initial solutions were composed of $TiCl_4$:EtOH:F127:H_2O mixtures, with a 1:40:0.005:10 molar ratio of the reagents. These solutions were used freshly after preparation (no ageing). In the case of mesoporous silica films the mixture TEOS:EtOH:F127:H_2O:HCl was prepared with a ratio 1:40:0.005:10:0.008. Silica precursor solutions were aged for 72h at room temperature prior to utilization. Silica and titania films are labeled SF and TF respectively, where F represents the surfactant template F127 used to texture the mesoporous films. After spin coating, the films were placed in 50% relative humidity chambers (obtained with a NaBr saturated solution) for

24h and subjected to a stabilizing thermal treatment procedure comprising two successive 24h heat treatments at 60 and 120 ºC, and a final step at 200 ºC for 2h. The template was finally eliminated by immersing the films in ethanol for 3 days.

Nanoparticle seeded growth. The growth of the Au nanoparticles embedded in mesoporous films was carried out by immersing the composite film in a solution containing $HAuCl_4$, CTAB and AA. In the case of gold nanoparticles covered with a titania mesoporous film, the concentration of $HAuCl_4$ in the growth solution was 6.25×10^{-5} M, the AA:Au molar ratio was varied between 2 and 32 and the CTAB:Au molar ratio was varied between 30 and 120. For the substrates with 80 nm GNPs and the 15nmGNP@SF substrate the growth solution was composed of an Au/CTAB/AA mixture with a molar ratio of 1:60:16 ([Au]= 6.25×10^{-5} M). Films were removed from the growth solution every 2 hours of reaction. After each growth step the films were washed and dried in air.

Characterization. UV-vis-NIR spectra were recorded using an Agilent 8453 spectrophotometer. Transmission electron microscopy (TEM) analysis was performed by using a JEOL JEM 1010 microscope operating at an acceleration voltage of 100 kV. Samples for TEM were obtained by scratching the films from the substrate and depositing them on carbon and FORMVAR-coated copper grids. Refractive index values of mesoporous thin films were obtained from spectroscopic ellipsometry measurements performed with a SE SOPRA GES5A setup, analyzed using an appropriate model, according to each oxide. Measurements were performed in ambient conditions (RH ~ 50%, temperature ~ 25ºC). SERS experiments were conducted with a Renishaw InVia Reflex system. The spectrograph used high-resolution gratings (1200 or 1800 grooves mm^{-1}) with additional bandpass-filter optics. Several laser excitation

energies were employed, including laser lines at 633 (HeNe), 785 and 830 nm (diode). All measurements were made in a confocal microscope in backscattering geometry using a 50× objective with a numerical aperture (NA) value of 0.75, which provided scattering areas of ≈1 μm^2. For SERS measurements, film fragments of about 0.5×0.5 cm^2 were immersed overnight in 10^{-5}M 4-NBT solutions (solvent: phosphate buffer solution; PBS pH 7.4) and air-dried. The power at the sample was maintained as low as ≈1 μW.

Size- exclusion experiments. Fragments (ca. 0.5×0.5 cm^2) of Sample 8 were immersed in solutions with and without 4-NBT (10^{-5} M) in BSA (50 mg mL^{-1}), which was also used as blank solution. The 4-NBT solution was also prepared in BSA (50 mg mL^{-1}), and the BSA solution was prepared in PBS 7.4. After immersion overnight, the samples were air-dried and SERS experiments were conducted in the Raman setup, using the laser excitation line of 785 nm. Spectra acquisition in extended mode of 30 points in each sample was carried out by using the Renishaw continuous grating mode. Time acquisition at each point was 25s with a laser power of ≈1 μW.

Acknowledgments

This work has been funded by the European Research Council (ERC Advanced Grant #267867 Plasmaquo) and the Spanish Ministerio de Economía y Competitividad (CTQ2011-23167). VL-P and SA-C respectively acknowledge FPI and FPU scholarships from the Spanish MINECO. PCA is a CONICET researcher.

Supporting Information Available: TEM images and UV-vis spectra for SF films. Comparison of SERS efficiencies for different samples. Effect of incubation in BSA for SF and TF films. Sieving proof-of-concept for 15nmGNPs. This material is available free of charge via the Internet at http://pubs.acs.org

References

(1) Alvarez-Puebla, R. A.; Liz-Marzán, L. M. SERS-Based Diagnosis and Biodetection. *Small* **2010,** *6*, 604-610.

(2) Alvarez-Puebla, R. A.; Agarwal, A.; Manna, P.; Khanal, B. P.; Aldeanueva-Potel, P.; Carbó-Argibay, E.; Pazos-Pérez, N.; Vigderman, L.; Zubarev, E. R.; Kotov, N. A., et al. Gold Nanorods 3D-Supercrystals as Surface Enhanced Raman Scattering Spectroscopy Substrates for the Rapid Detection of Scrambled Prions. *Proc. Natl. Acad. Sci. USA* **2011**, *108*, 8157-8161.

(3) Zhang, D.; Ansar, S. M.; Vangala, K.; Jiang, D. Protein Adsorption Drastically Reduces Surface-Enhanced Raman Signal of Dye Molecules. *J. Raman Spectrosc.* **2010,** *41*, 952-957.

(4) Li, W.; Zhao, D. An Overview of the Synthesis of Ordered Mesoporous Materials. *Chem. Commun.* **2013,** *49*, 943-946.

(5) Sanchez, C.; Boissière, C.; Grosso, D.; Laberty, C.; Nicole, L. Design, Synthesis, and Properties of Inorganic and Hybrid Thin Films Having Periodically Organized Nanoporosity. *Chem. Mater.* **2008,** *20*, 682-737.

(6) Soler-Illia, G. J. d. A. A.; Sanchez, C.; Lebeau, B.; Patarin, J. Chemical Strategies To Design Textured Materials: from Microporous and Mesoporous Oxides to Nanonetworks and Hierarchical Structures. *Chem. Rev.* **2002,** *102*, 4093-4138.

(7) Calvo, A.; Fuertes, M. C.; Yameen, B.; Williams, F. J.; Azzaroni, O.; Soler-Illia, G. J. A. A. Nanochemistry in Confined Environments: Polyelectrolyte Brush-Assisted Synthesis of Gold Nanoparticles inside Ordered Mesoporous Thin Films. *Langmuir* **2010,** *26*, 5559-5567.

(8) Andersson, M.; Birkedal, H.; Franklin, N. R.; Ostomel, T.; Boettcher, S.; Palmqvist, A. E. C.; Stucky, G. D. Ag/AgCl-Loaded Ordered Mesoporous Anatase for Photocatalysis. *Chem. Mater.* **2005,** *17*, 1409-1415.

(9) Fuertes, M. C.; Marchena, M.; Marchi, M. C.; Wolosiuk, A.; Soler-Illia, G. J. A. A. Controlled Deposition of Silver Nanoparticles in Mesoporous Single- or Multilayer Thin Films: From Tuned Pore Filling to Selective Spatial Location of Nanometric Objects. *Small* **2009,** *5*, 272-280.

(10) Martínez, E. D.; Bellino, M. n. G.; Soler-Illia, G. J. A. A. Patterned Production of Silver−Mesoporous Titania Nanocomposite Thin Films Using Lithography-Assisted Metal Reduction. *ACS Appl. Mater. Interf.* **2009,** *1*, 746-749.

(11) Pérez, M. D.; Otal, E.; Bilmes, S. A.; Soler-Illia, G. J. A. A.; Crepaldi, E. L.; Grosso, D.; Sanchez, C. Growth of Gold Nanoparticle Arrays in TiO2 Mesoporous Matrixes. *Langmuir* **2004,** *20*, 6879-6886.

(12) Plyuto, Y.; Berquier, J.-M.; Jacquiod, C.; Ricolleau, C. Ag Nanoparticles Synthesised in Template-Structured Mesoporous Silica Films on a Glass Substrate. *Chem. Commun.* **1999**, 1653-1654.

(13) Wang, H.-W.; Lin, H.-C.; Kuo, C.-H.; Cheng, Y.-L.; Yeh, Y.-C. Synthesis and Photocatalysis of Mesoporous Anatase TiO2 Powders Incorporated Ag Nanoparticles. *J. Phys. Chem. Solids* **2008,** *69*, 633-636.

(14) Zhu, J.; Kónya, Z.; Puntes, V. F.; Kiricsi, I.; Miao, C. X.; Ager, J. W.; Alivisatos, A. P.; Somorjai, G. A. Encapsulation of Metal (Au, Ag, Pt) Nanoparticles into the Mesoporous SBA-15 Structure. *Langmuir* **2003,** *19*, 4396-4401.

(15) Walters, G.; Parkin, I. P. The Incorporation of Noble Metal Nanoparticles into Host MatrixThin Films: Synthesis, Characterisation and Applications. *J. Mater. Chem.* **2009,** *19*, 574-590.

(16) Zhang, X.; Zhao, J.; Whitney, A. V.; Elam, J. W.; Van Duyne, R. P. Ultrastable Substrates for Surface-Enhanced Raman Spectroscopy: Al_2O_3 Overlayers Fabricated by Atomic Layer Deposition Yield Improved Anthrax Biomarker Detection. *J. Am. Chem. Soc.* **2006,** *128*, 10304-10309.

(17) Dong, J.; Tao, Q.; Guo, M.; Yan, T.; Qian, W. Glucose-Responsive Multifunctional Acupuncture Needle: A Universal SERS Detection Strategy of Small Biomolecules in Vivo. *Anal. Methods* **2012,** *4*, 3879-3883.

(18) Petrova, H.; Perez Juste, J.; Pastoriza-Santos, I.; Hartland, G. V.; Liz-Marzan, L. M.; Mulvaney, P. On the Temperature Stability of Gold Nanorods: Comparison between Thermal and Ultrafast Laser-Induced Heating. *Phys. Chem. Chem. Phys.* **2006,** *8*, 814-821.

(19) Angelome, P. C.; Pastoriza-Santos, I.; Perez-Juste, J.; Rodriguez-Gonzalez, B.; Zelcer, A.; Soler-Illia, G. J. A. A.; Liz-Marzan, L. M. Growth and Branching of Gold Nanoparticles through Mesoporous Silica Thin Films. *Nanoscale* **2012,** *4*, 931-939.

(20) Barbosa, S.; Agrawal, A.; Rodríguez-Lorenzo, L.; Pastoriza-Santos, I.; Alvarez-Puebla, R. A.; Kornowski, A.; Weller, H.; Liz-Marzán, L. M. Tuning Size and Sensing Properties in Colloidal Gold Nanostars. *Langmuir* **2010,** *26*, 14943-14950.

(21) Alvarez-Puebla, R. A.; Liz-Marzán, L. M.; García de Abajo, F. J. Light Concentration at the Nanometer Scale. *J. Phys. Chem. Lett.* **2010,** *1*, 2428-2434.

(22) Rodriguez-Lorenzo, L.; Alvarez-Puebla, R. A.; Pastoriza-Santos, I.; Mazzucco, S.; Stephan, O.; Kociak, M.; Liz-Marzan, L. M.; Garcia de Abajo, F. J. Zeptomol Detection Through Controlled Ultrasensitive Surface-Enhanced Raman Scattering. *J. Am. Chem. Soc.* **2009,** *131*, 4616-4618.

(23) Wang, F.; Widejko, R. G.; Yang, Z.; Nguyen, K. T.; Chen, H.; Fernando, L. P.; Christensen, K. A.; Anker, J. N. Surface-Enhanced Raman Scattering Detection of pH with Silica-Encapsulated 4-Mercaptobenzoic Acid-Functionalized Silver Nanoparticles. *Anal. Chem.* **2012,** *84*, 8013-8019.

(24) Scarpettini, A. F.; Bragas, A. V. Coverage and Aggregation of Gold Nanoparticles on Silanized Glasses. *Langmuir* **2010,** *26*, 15948-15953.

(25) Angelomé, P. C.; Liz-Marzán, L. M. Monitoring Solvent Evaporation from Thin Films by Localized Surface Plasmon Resonance Shifts. *J. Phys. Chem. C* **2010,** *114*, 18379-18383.

(26) Crepaldi, E. L.; Soler-Illia, G. J. d. A. A.; Grosso, D.; Cagnol, F.; Ribot, F.; Sanchez, C. Controlled Formation of Highly Organized Mesoporous Titania Thin Films: From Mesostructured Hybrids to Mesoporous Nanoanatase TiO2. *J. Am. Chem. Soc.* **2003,** *125*, 9770-9786.

(27) Kumar, P. S.; Pastoriza-Santos, I.; Rodríguez-González, B.; Abajo, F. J. G. d.; Liz-Marzán, L. M. High-Yield Synthesis and Optical Response of Gold Nanostars. *Nanotechnology* **2008,** *19*, 015606.

(28) Bass, J. D.; Grosso, D.; Boissiere, C.; Belamie, E.; Coradin, T.; Sanchez, C. Stability of Mesoporous Oxide and Mixed Metal Oxide Materials under Biologically Relevant Conditions. *Chem. Mater.* **2007,** *19*, 4349-4356.

(29) Skadtchenko, B. O.; Aroca, R. Surface-Enhanced Raman Scattering of p-Nitrothiophenol: Molecular Vibrations of its Silver Salt and the Surface Complex Formed on Silver Islands and Colloids. *Spectrochim. Acta, Part A* **2001,** *57*, 1009-1016.

(30) Alvarez-Puebla, R. A.; Liz-Marzán, L. M. SERS Detection of Small Inorganic Molecules and Ions. *Angew. Chem. Int. Ed.* **2012,** *51*, 11214-11223.

(31) Pazos-Perez, N.; Garcia de Abajo, F. J.; Fery, A.; Alvarez-Puebla, R. A. From Nano to Micro: Synthesis and Optical Properties of Homogeneous Spheroidal Gold Particles and Their Superlattices. *Langmuir* **2012,** *28*, 8909-8914.

(32) Aldeanueva-Potel, P.; Carbó-Argibay, E.; Pazos-Pérez, N.; Barbosa, S.; Pastoriza-Santos, I.; Alvarez-Puebla, R. A.; Liz-Marzán, L. M. Spiked Gold Beads as Substrates for Single-Particle SERS. *ChemPhysChem* **2012,** *13*, 2561-2565.

(33) Thomas, G. J. Raman Spectroscopy of Protein and Nucleic Acid Assemblies. *Annu. Rev. Biophys. Biomol. Struct.* **1999,** *28*, 1-27.

(34) Tuma, R. Raman Spectroscopy of Proteins: From Peptides to Large Assemblies. *J. Raman Spectrosc.* **2005,** *36*, 307-319.

(35) Boissiere, C.; Grosso, D.; Lepoutre, S.; Nicole, L.; Bruneau, A. B.; Sanchez, C. Porosity and Mechanical Properties of Mesoporous Thin Films Assessed by Environmental Ellipsometric Porosimetry. *Langmuir* **2005,** *21*, 12362-12371.

(36) Soler-Illia, G. J. A. A.; Angelome, P. C.; Fuertes, M. C.; Grosso, D.; Boissiere, C. Critical Aspects in the Production of Periodically Ordered Mesoporous Titania Thin Films. *Nanoscale* **2012,** *4*, 2549-2566.

(37) Turkevich, J.; Stevenson, P. C.; Hillier, J. A Study of the Nucleation and Growth Processes in the Synthesis of Colloidal Gold. *Discuss. Faraday Soc.* **1951,** *11*, 55-75.

(38) Bastús, N. G.; Comenge, J.; Puntes, V. Kinetically Controlled Seeded Growth Synthesis of Citrate-Stabilized Gold Nanoparticles of up to 200 nm: Size Focusing versus Ostwald Ripening. *Langmuir* **2011,** *27*, 11098-11105.

(39) Grosso, D.; Balkenende, A. R.; Albouy, P. A.; Ayral, A.; Amenitsch, H.; Babonneau, F. Two-Dimensional Hexagonal Mesoporous Silica Thin Films

Prepared from Block Copolymers: Detailed Characterization and Formation Mechanism. *Chem. Mater.* **2001,** *13*, 1848-1856.

(40) Soler-Illia, G. J. A. A.; Angelome, P. C.; Fuertes, M. C.; Grosso, D.; Boissiere, C. Critical Aspects in the Production of Periodically Ordered Mesoporous Titania Thin Films. *Nanoscale* **2012,** *4*, 2549-2566.